SUPPLEMENT ARTICLE

Amino Acid Residue at Position 79 of Marburg Virus VP40 Confers Interferon Antagonism in Mouse Cells

Alicia R. Feagins and Christopher F. Basler

Department of Microbiology, Icahn School of Medicine at Mount Sinai, New York, New York

Marburg viruses (MARVs) cause highly lethal infections in humans and nonhuman primates. Mice are not generally susceptible to MARV infection; however, if the strain is first adapted to mice through serial passaging, it becomes able to cause disease in this animal. A previous study correlated changes accrued during mouse adaptation in the VP40 gene of a MARV strain known as Ravn virus (RAVV) with an increased capacity to inhibit interferon (IFN) signaling in mouse cell lines. The MARV strain Ci67, which belongs to a different phylogenetic clade than RAVV, has also been adapted to mice and in the process the Ci67 VP40 acquired a different collection of genetic changes than did RAVV VP40. Here, we demonstrate that the mouse-adapted Ci67 VP40 more potently antagonizes IFN-α/β–induced STAT1 and STAT2 tyrosine phosphorylation, gene expression, and antiviral activity in both mouse and human cell lines, compared with the parental Ci67 VP40. Ci67 VP40 is also demonstrated to target the activation of kinase Jak1. A single change at VP40 residue 79 was found to be sufficient for the increased VP40 IFN antagonism. These data argue that VP40 IFN-antagonist activity plays a key role in MARV pathogenesis in mice.

Keywords. Marburg virus; Ravn virus; Ci67 strain; VP40; interferon; mouse-adapted.

Marburg virus (MARV), a member of the *Filoviridae* family along with the Ebola viruses (EBOVs), is the etiological agent of MARV disease [1–3]. The high mortality rate associated with filovirus disease is likely due, in part, to viral encoded proteins that effectively inhibit the host antiviral responses [4]. Upon viral infection, pattern-recognition receptors recognize virus pathogen-associated molecular patterns and trigger a signaling cascade that culminates in the production of interferon α/β (IFN-α/β). The IFN-α/βs then bind to the IFN-α/β receptor to activate JAK1 and TYK2 Janus kinases. The activated kinases phosphorylate STAT1 and STAT2, which dimerize, translocate to the nucleus, and stimulate transcription of hundreds of IFN-stimulated genes (ISGs) and the establishment of an antiviral state [5].

Correspondence: Christopher F. Basler, PhD, Icahn School of Medicine at Mount Sinai, Department of Microbiology, Box 1124, 1 Gustave L. Levy Pl, New York, NY 10029 (chris.basler@mssm.edu).

The Journal of Infectious Diseases® 2015;212:S219–25

DOI: 10.1093/infdis/jiv010

Filoviral proteins, including both MARV and EBOV, block particular aspects of the IFN responses [6–9]. The VP35 proteins of MARV and EBOV impair the production of IFN-α/β by antagonizing the RIG-I signaling pathway [10–13]. EBOV VP24 blocks IFN-α/β and IFN-γ signaling by interacting with karyopherin α proteins to prevent the nuclear accumulation of tyrosine phosphorylated STAT1 [14–17]. In contrast, the MARV VP24 protein does not antagonize IFN responses. Rather, it modulates antioxidant responses through interaction with host protein Keap1 [18]. Instead, MARV uses its VP40 matrix protein to inhibit Jak1 and block IFN-α/β, IFN-γ, and interleukin 6 signaling [19].

Inhibition of IFN signaling by the VP40 protein was previously linked to host range and virulence in mice. Previously, Ravn virus (RAVV) was serially passaged in mice to produce mouse-adapted RAVV (maRAVV) and a lethal model of MARV disease [20, 21]. A number of changes were acquired throughout the genome during mouse adaptation, with 7 amino acid changes occurring in VP40, the viral matrix protein and IFN antagonist [21]. Interestingly, maRAVV VP40 was demonstrated to inhibit IFN signaling in both mouse and

human cells, whereas RAVV VP40 inhibited IFN signaling in human cells but not mouse cells [22]. Subsequent mapping experiments revealed that 2 changes associated with mouse adaptation, V57A and D165A, were sufficient for RAVV VP40 to inhibit JAK/STAT signaling in mouse cells [22].

The Ci67 strain of MARV was also passaged in mice until lethality was achieved [21]. VP40 acquired 5 mutations during this adaptation: Y19H, G79S, D184N, I187T, and I228M. Surprisingly, the 2 mutations critical for RAVV VP40 IFN antagonism in mouse cells were not among the mutations that Ci67 acquired. Therefore, it was of interest to characterize the IFN-antagonist function of maCi67 VP40. Here, we demonstrate that maCi67 VP40, like maRAVV VP40, inhibits IFN signaling in both human and mouse cells, whereas the parental Ci67 VP40 effectively inhibits IFN signaling only in human cells. Additionally, amino acids critical for Ci67 to inhibit IFN signaling in mouse cells were identified, and these residues differ from those identified in RAVV VP40. The reproducible coupling of increased VP40 IFN antagonist function with increased mouse virulence suggests that VP40 IFN-antagonist function may be a critical virulence determinant in mice.

MATERIALS AND METHODS

Cells and Viruses

293T, Huh7 (human liver), Hepa1.6 (mouse liver), and STAT2$^{-/-}$ mouse embryonic fibroblast (MEF) cells were maintained in Dulbecco's modified Eagle's medium (DMEM; Invitrogen) supplemented with 10% fetal bovine serum (Invitrogen) and grown at 37°C in the presence of 5% CO_2. Newcastle disease virus expressing green fluorescent protein (NDV-GFP) was described previously [23].

Plasmids

FLAG-tagged MARV and Langat virus (LGTV) NS5 viral protein expression plasmids were described previously [19, 22]. The MARV Ci67 VP40 mutants were constructed using the QuikChange II XL site-directed mutagenesis kit (Stratagene). Human JAK1, mouse JAK1, and mouse STAT2 were also described previously [19, 22].

Transfections

All transfections were performed with Lipofectamine 2000 (Invitrogen) at a ratio of 1:1, 1:2.75, 1:3, or 1:2 with plasmid DNA for 293T, Huh7, Hepa1.6, or STAT2$^{-/-}$ MEF cells, respectively, following the manufacturer's protocol.

Interferon Treatments

Cells were treated with 1000 IU/mL of universal IFN (PBL) for 30 minutes in Roswell Park Memorial Institute 1640 medium supplemented with 0.3% bovine serum albumin.

ISG54 Reporter Gene Assay

Hepa1.6 and Huh7 cells were seeded in a 24-well plate and cotransfected with empty vector (pCAGGS) or the indicated virus protein expression plasmids, a plasmid that constitutively expresses *Renilla* luciferase, and a reporter plasmid expressing firefly luciferase gene under control of the ISG54 promoter. Twenty-four hours after transfection, cells were treated with 1000 IU/mL of IFN for 24 hours. Cells were then lysed and luciferase activity was assessed using a dual luciferase kit (Promega) according to the manufacturer's protocol. Each sample was assayed in triplicate.

NDV-GFP Bioassay

The NDV-GFP assay was performed as described previously [22]. Briefly, 6-well plates were seeded with Hepa1.6 cells and transfected with the indicated expression plasmids. Twenty-four hours after transfection, cells were infected with NDV-GFP at a multiplicity of infection of 10 in DMEM supplemented with 10% fetal bovine serum. Fifteen hours after infection, cells were harvested and prepared for fluorescence-activated cell sorting (FACS). Data were analyzed using FlowJo software.

Western Blotting

Transfected cells were washed with phosphate-buffered saline and lysed in radioimmunoprecipitation assay buffer (50 mM Tris [pH 7.4], 150 mM NaCl, 0.1% sodium dodecyl sulfate [SDS], 0.5% deoxycholate, and 1% NP-40) supplemented with PhosSTOP phosphatase inhibitor (Roche) and cOmplete protease inhibitor cocktail (Roche). Lysates were analyzed by SDS-polyacrylamide gel electrophoresis and visualized by Western blot to detect viral proteins (anti-FLAG M2; Sigma), tyrosine phosphorylated STAT1 (mouse anti-pY701 STAT1; BD Transduction Laboratories), total STAT1 (mouse anti-STAT1; BD Transduction Laboratories), tyrosine phosphorylated STAT2 (rabbit anti-pY689 STAT2; Millipore), tyrosine phosphorylated JAK1 (rabbit anti-JAK1; Santa Cruz), JAK1 (mouse anti-JAK1; Cell Signaling), and β-tubulin (mouse anti-β-tubulin; Sigma). Protein levels for transfected Flag-STAT2 were detected with anti-FLAG antibody M2 (Sigma).

Statistical Analysis

All statistical analysis was performed using GraphPad Prism software. Columns represent the mean and error bars represent the standard deviation of triplicate samples and statistical significance was assessed by a Student *t* test.

RESULTS

maCi67 VP40 Inhibits IFN Signaling in Mouse and Human Cells

The phosphorylation of STAT1 and STAT2 is a critical early step in IFN signaling. To compare the capacity of the parental Ci67 VP40 and the mouse-adapted Ci67 VP40 (maVP40) to

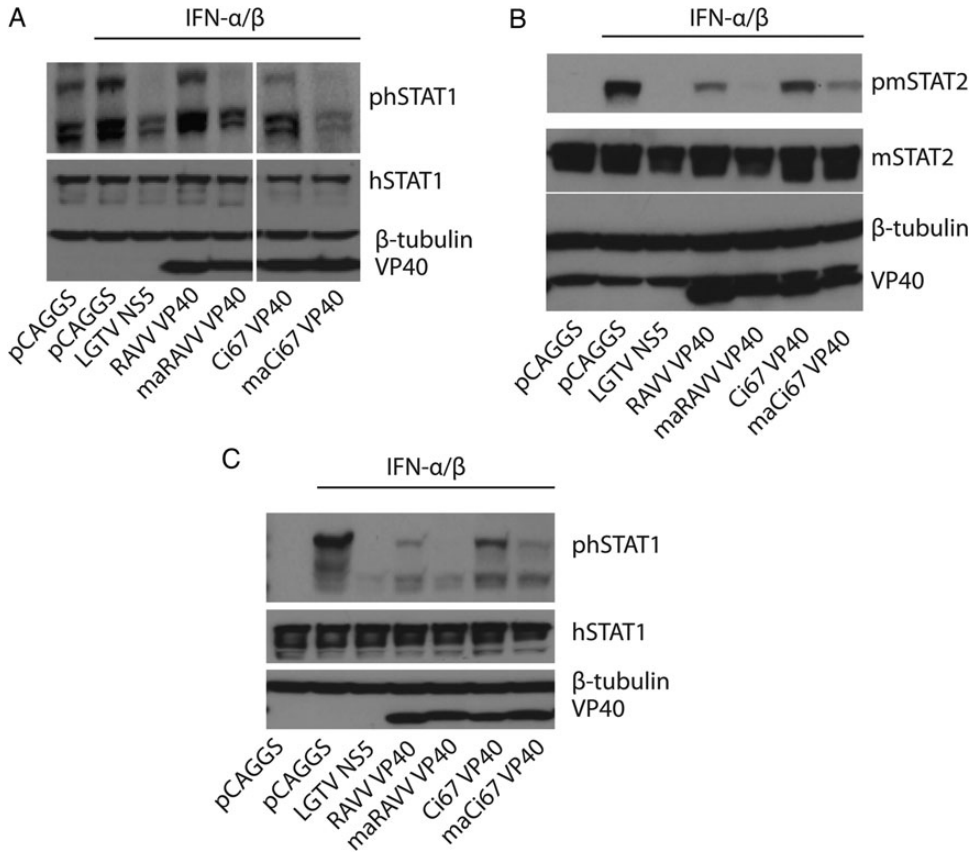

Figure 1. maCi67 VP40 exhibits enhanced inhibition of interferon (IFN) signaling in mouse and human cells. *A* and *B*, Hepa1.6 cells overexpressing STAT1–green fluorescent protein (GFP; *A*) or STAT2$^{-/-}$ mouse embryonic fibroblasts overexpressing mouse STAT2-GFP (*B*) were transfected with the indicated expression plasmids. Twenty-four hours after transfection, cells were treated with IFN (1000 IU/mL) for 30 minutes. Cells were subsequently lysed and analyzed by Western blot for total and tyrosine phosphorylated STAT1 and STAT2 phosphorylation, respectively. *C*, 293T cells overexpressing STAT1-GFP were transfected, treated with IFN, and lysed as described above. Cell lysates were analyzed by Western blot for total STAT1 and for tyrosine phosphorylated STAT1. Lysates were also probed for β-tubulin as a loading control and with anti-Flag antibody to detect Flag-tagged VP40s.

antagonize IFN signaling, we examined STAT1 and STAT2 tyrosine phosphorylation following IFN-α/β addition to transfected mouse cell lines. For these studies, empty vector (pCAGGS) served as a negative control. The previously described IFN signaling inhibitor, Langat virus NS5 protein, served as a positive control [24]. Also included were the RAVV parental and mouse-adapted VP40 proteins. In Hepa1.6 cells overexpressing STAT1-GFP, which typically runs as multiple bands on our Western blots, the parental Ci67 VP40 only modestly affected tyrosine phosphorylation of STAT1, while the maCi67 VP40 exhibited an enhanced ability to inhibit STAT1 phosphorylation, comparable to the inhibition seen with LGTV NS5. The enhanced activity of maCi67 VP40 was very similar to the enhanced activity of maRAVV VP40 versus that of the parental RAVV VP40 (Figure 1*A*). We next assessed IFN-induced STAT2 phosphorylation in the presence of maCi67 VP40 expression in STAT2$^{-/-}$ MEF cells that were transfected with a Flag-tagged mouse STAT2 expression plasmid. The maCi67 VP40 significantly inhibited STAT2 phosphorylation when compared to Ci67 VP40 (Figure 1*B*). Despite the dramatic differences in suppression of STAT1 and STAT2 phosphorylation in mouse cell lines, both the parental and maCi67 VP40 decreased STAT1 tyrosine phosphorylation in the human-derived 293T cell line that had been transfected with a STAT1 expression plasmid (Figure 1*C*). Interestingly, in both cases, suppression of STAT1 tyrosine phosphorylation was more complete in the presence of the mouse-adapted VP40.

IFN-induced tyrosine phosphorylated STAT1 and STAT2 heterodimerize, interact with IRF9, and accumulate in the nucleus, where the transcription factor complex activates expression of ISGs. To determine whether maCi67 VP40 inhibits IFN-induced gene expression in mouse and human cells, reporter gene assays measuring IFN-induced activation of the ISG54 promoter were performed in either Hepa1.6 or Huh7 cells. Activation was blocked in both cell types by maCi67 VP40 and to a greater extent than parental Ci67 VP40 (Figure 2*A* and 2*B*). A similar pattern of suppression was seen with parental and mouse-adapted RAVV VP40. Therefore,

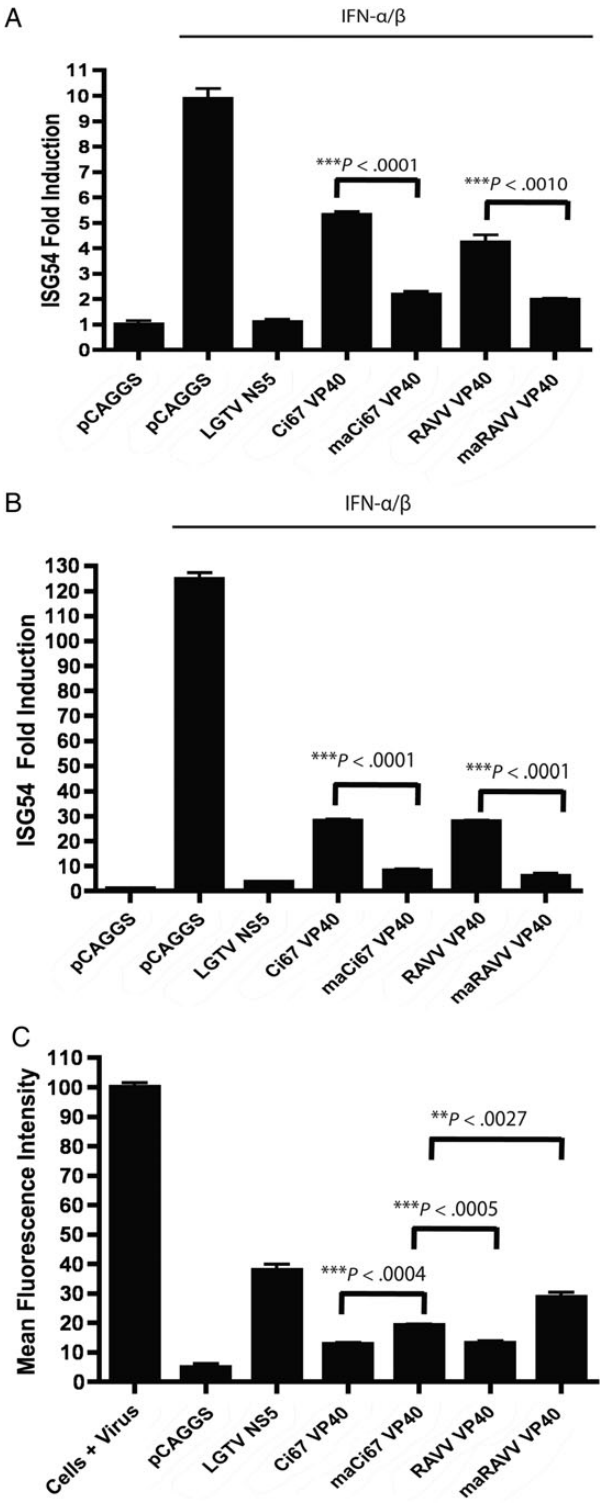

Figure 2. Expression of maCi67 VP40 inhibits interferon α/β (IFN-α/β)–induced ISG54 promoter activation in mouse and human cells and counteracts the antiviral response in mouse cells. *A* and *B*, Hepa1.6 cells (*A*) and Huh7 cells (*B*) were cotransfected with the indicated expression plasmids, a plasmid expressing *Renilla* luciferase, and a reporter plasmid expressing firefly luciferase gene under control of the ISG54 promoter. Twenty-four hours after transfection, cells were mock treated or treated with IFN-α/β (1000 IU/mL) for 24 hours. Cells were subsequently lysed, and a dual luciferase assay was performed. Firefly luciferase activity was normalized to *Renilla* luciferase activity. Each sample was assayed in triplicate, and bars represent the mean fold induction. *C*, Hepa1.6 cells were mock-transfected or transfected with the indicated expression plasmids. Twenty-four hours after transfection, cells were infected with Newcastle disease virus expressing green fluorescent protein (GFP) at a multiplicity of infection of 10. Fifteen hours after infection, cells were analyzed by flow cytometry to determine the mean fluorescence intensity of the GFP signal. Each sample was assayed in triplicate; columns represent the mean fluorescence intensity, and error bars represent the standard deviations. The 1-tailed Student *t* test was used to calculate *P* values, using the GraphPad Prism software.

mouse adaptation increased the ability of VP40s to suppress IFN-induced gene expression in both the mouse and the human cell line.

Expression of maCi67 VP40 Counteracts the Antiviral Response in Mouse Cells

We next assessed whether the expression of maCi67 VP40 can counteract the host antiviral response and thereby enhance viral replication. Hepa1.6 cells were mock transfected or transfected with pCAGGS, LGTV NS5, Ci67 VP40, maCi67 VP40, and the previously characterized RAVV and maRAVV VP40s. Twenty-four hours after transfection, the cells were infected with NDV-GFP at a multiplicity of infection of 10 and subsequently analyzed by FACS for GFP expression, which serves as an indicator of virus replication. Valmas et al previously demonstrated that the transfection of empty vector (pCAGGS) alone in Hepa1.6 cells is sufficient to induce IFN-α/β production and signaling [22]. As a result, an antiviral state is established which then restricts NDV-GFP replication and inhibits GFP expression (Figure 2*C*). The expression of LGTV NS5, a potent IFN antagonist, counteracted the antiviral response and enhanced the replication of NDV GFP. maCi67 VP40 counteracted the antiviral response in a manner similar to maRAVV VP40, albeit to a lesser extent. Recovery of NDV-GFP replication by maCi67 VP40 expression was significantly greater than that observed with the expression of parental Ci67 VP40, and the recovery was similar in magnitude to that observed for maRAVV VP40 (Figure 2*C*).

maCi67 VP40 Antagonizes IFN Signaling at the Level of JAK1 Phosphorylation

RAVV VP40 was previously demonstrated to inhibit Jak1 activation [19]. In mouse Hepa1.6 cells overexpressing JAK1, maCi67 inhibited JAK1 tyrosine phosphorylation comparably to maRAVV VP40. In contrast, parental Ci67 VP40 and RAVV VP40 were less effective at reducing the phosphorylation of JAK1 (Figure 3*A*). In human-derived 293T cells overexpressing human JAK1, both maCi67 and parental Ci67 VP40s inhibited JAK1 phosphorylation in a similar manner to RAVV and maRAVV VP40, respectively (Figure 3*B*). Because the inhibition was

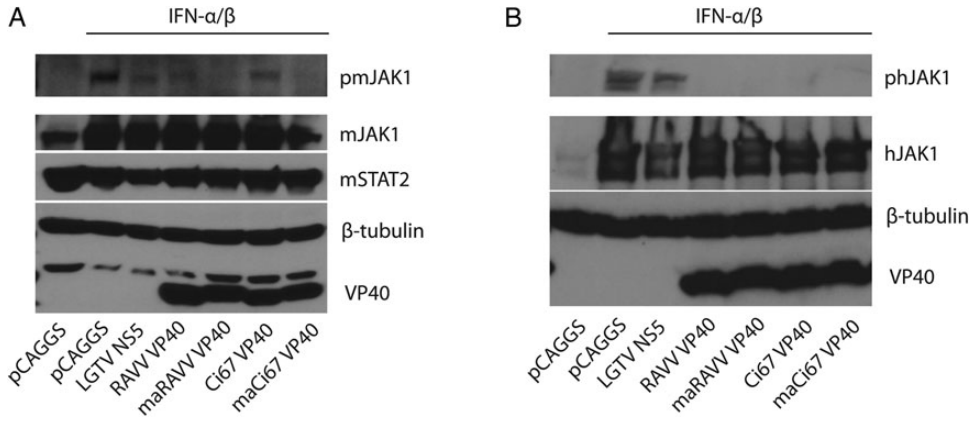

Figure 3. maCi67 VP40 antagonizes interferon (IFN) signaling at the level of JAK1 phosphorylation. *A* and *B*, STAT2$^{-/-}$ mouse embryonic fibroblasts overexpressing STAT2 (*A*) and 293T cells (*B*) were cotransfected with mouse and human JAK1 FLAG, respectively, and the indicated additional expression plasmids. Twenty-four hours after transfection, cells were treated with IFN (1000 IU/mL) for 30 minutes. Cells were subsequently lysed and analyzed for total and tyrosine phosphorylated JAK1, for β-tubulin, and for the transfected Flag-tagged VP40s, which were detected with anti-Flag antibody.

complete under the conditions tested, we could not determine whether the various VP40s exhibited differential inhibition of Jak1 in the 293T cells. Taken together, the data suggest that maCi67 VP40 inhibits IFN signaling at or above the level of Jak1.

Mutating Amino Acid 79 of Ci67 VP40 Enhances IFN Antagonism in Mouse Cells

Five amino acid mutations were acquired in Ci67 VP40 during mouse adaptation. To identify the residues critical for IFN antagonism, single residues in the Ci67 VP40 were mutated to reflect changes seen after mouse adaptation. Specifically, Ci67 VP40 Y19H, G79S, D184N, I187T, and I228 mutants were constructed. These variants were tested in STAT2$^{-/-}$ MEFs overexpressing mouse STAT2 for inhibition of IFN-α/β–induced STAT2 tyrosine phosphorylation. Mutating positions 19, 184, or 187 modestly enhanced Ci67 VP40 inhibition of STAT2 phosphorylation in the mouse cell line to levels comparable to that observed with maCi67 VP40. Interestingly, replacing the glycine at position 79 of Ci67 VP40 with a serine resulted in an enhanced IFN-antagonist function relative to maCi67 VP40 (Figure 4).

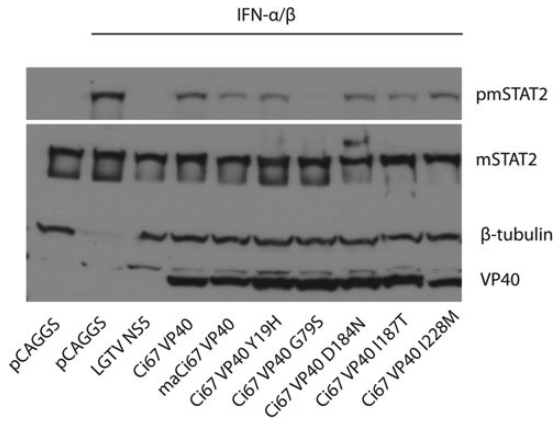

Figure 4. Mutating amino acid 79 of Ci67 VP40 enhances interferon (IFN) antagonism in mouse cells. STAT2$^{-/-}$ mouse embryonic fibroblasts overexpressing STAT2–green fluorescent protein (GFP) were transfected with the indicated expression plasmids. Twenty-four hours after transfection, cells were IFN treated (1000 IU/mL) for 30 minutes. Cells were subsequently lysed and analyzed for total and tyrosine phosphorylated STAT2. Lysates were also probed for β-tubulin as a loading control and with anti-Flag antibody to detect Flag-tagged VP40s.

DISCUSSION

Filoviruses do not cause death in adult immunocompetent mice or guinea pigs unless adapted to these species first. Therefore, mouse- and guinea pig–adapted MARV and EBOV have been developed by serial passage in these species [20, 21, 25–29]. Our previous work demonstrated that changes occurring in MARV VP40 during adaptation to mice enhanced MARV VP40 IFN-antagonist function [22]. Specifically, RAVV VP40, a protein previously characterized as a MARV IFN antagonist [19], acquired 7 amino acid changes during mouse adaptation of the virus: Y7H, Y19H, V57A, T165A, D184N, N189S, and T190A [21]. Valmas et al demonstrated that maRAVV VP40 exhibited increased IFN-antagonist function in mouse cell lines, and 2 of the mutations, V57A and T165A, were found to be sufficient for the increased IFN antagonism in mouse cells [22]. This suggested a link between mouse virulence and IFN-antagonist function. Lofts et al also adapted the MARV Ci67 strain to mice and assessed the resulting genomic changes [21]. The sequences from this study allowed us to ask whether a similar phenomenon occurred in this second case of mouse adaptation.

In the present study, we provide several lines of evidence indicating that mouse adaptation also altered the IFN-antagonist

function of the Ci67 VP40. Interestingly, mouse adaptation appears to enhance IFN-antagonist function in both human and mouse-derived cell lines. We reached the same conclusion when examining the effects of VP40s on distinct steps of the IFN-α/β signaling pathway. In 2 different mouse cell lines, Hepa1.6 and STAT2$^{-/-}$ MEFs reconstituted with STAT2 by transfection, the parental Ci67 VP40 and the parental RAVV VP40 inhibited IFN-α/β–induced STAT1 or STAT2 tyrosine phosphorylation, relative to the IFN-treated empty vector control. However, both mouse-adapted versions of VP40 more completely suppressed STAT1/2 tyrosine phosphorylation. A similar pattern was seen in the human-derived 293T cell line. Similarly, when the same VP40s were tested for suppression of IFN-α/β–induced gene expression, the parental VP40s were weak inhibitors of ISG54 promoter activation, whereas in Hepa1.6 cells, the mouse-adapted VP40 exhibited improved suppression. In 293T cells, the parental VP40s exhibited somewhat more-robust inhibition, but mouse adaptation once again improved inhibitory function. These data would argue that mouse adaption alters the VP40 of either of 2 strains of MARV such that the IFN-antagonist function is improved in either mouse or human cells. However, because the parental VP40s are relatively ineffective inhibitors in mouse cells but already efficient in the human cells, the impact of adaptation is more dramatic in the mouse system.

Although MARV VP40 was previously demonstrated to inhibit Jak1 phosphorylation and activation, how mouse adaptation might influence inhibition of Jak1 was not assessed [19, 22]. In the present study, we demonstrate in STAT2$^{-/-}$ MEFs that the parental VP40s modestly inhibit IFN-α/β–induced Jak1 tyrosine phosphorylation but the mouse-adapted RAVV and Ci67 VP40s exhibit enhanced inhibitory activity. In the 293T cells, inhibition of Jak1 phosphorylation was sufficiently strong that no phospho-Jak1 was detected in any of the VP40-expressing cells. Therefore, our assay did not permit us to evaluate the relative strength of inhibition for the different VP40 variants. The RAVV and Ci67 VP40s are 98.7% identical at the amino acid level, differing at only 4 amino acid positions. Therefore, it is striking that different residues were selected for in the maCi67 VP40 (79) and maRAVV VP40 (57 and 165) but that, in each case, the changes allowed effective suppression of the antiviral response in mice. That there is plasticity in how VP40 may achieve increased IFN antagonism is further supported by the observation that the V57A and T165A changes that conferred an increased IFN antagonism to RAVV VP40 in mouse cells could also enhance the IFN-antagonist function of VP40 with the Ci67 sequence [22].

Another notable feature of the present study is that the impact on IFN-antagonist function is not restricted to mouse cells, with both the RAVV and Ci67 mouse-adapted VP40s exhibiting improved function in the 293T cells and in the mouse cell lines. Acquisition of increased activity may have more consequence in mouse cells, where the parental VP40s appear to have poor inhibitory activity. Nonetheless, the data suggest that MARV could evolve more potent VP40 IFN-antagonist function upon infection of humans or nonhuman primates. It is possible that the other functions of VP40, which include critical viral assembly and egress functions, constrain evolution of the IFN-antagonist function. In support of this, we recently reported that the valine at position 57 of RAVV VP40, which influences IFN-antagonist function, is critical for efficient VP40 budding from human but not mouse cell lines. Efficient budding from human cell lines correlates with relative resistance of VP40 to restriction by the IFN-induced antiviral protein tetherin. The identity of residue 57 also influences VP40 oligomerization, as assessed by coimmunoprecipitation assays [30].

The fact that mouse adaptation of 2 different MARV strains each time led to increased IFN-antagonist function in mouse cells suggests an important role for VP40 IFN-antagonist function in MARV virulence. It also suggests that this function should be explored as a target for anti-MARV therapeutics. Drugs targeting this function would be expected to augment the antiviral effects of IFNs produced during infection or given as a therapy. It will also be important in future studies to define the cellular targets of MARV VP40, to define how these host factors modulate Jak1 function and to understand from a structural point of view how various adaptive mutations alter IFN-antagonist activity.

Notes

Acknowledgment. We thank Christine Schwall for critical reading of the manuscript.

Financial support. This work was supported by the National Institutes of Health (grants R01AI059536, U19AI109945 [C. F. B., principle investigator], and U19AI109664 [C. F. B., principle investigator] to C. F. B.).

Potential conflict of interest. Both authors: No reported conflicts.

Both authors have submitted the ICMJE Form for Disclosure of Potential Conflicts of Interest. Conflicts that the editors consider relevant to the content of the manuscript have been disclosed.

References

1. Sanchez A, Geisbert TW, Feldmann H. Filoviridae: marburg and ebola viruses. In: Knipe DM, Howley PM, eds. Fields virology. 5th ed. Philadelphia: Lippincott Williams and Wilkins, **2007**:1410–48.
2. Paessler S, Walker DH. Pathogenesis of the viral hemorrhagic fevers. Annu Rev Pathol **2013**; 8:411–40.
3. World Health Organization. Marburg virus disease. **2014**. http://www.who.int/csr/disease/marburg/en/.
4. Martinez O, Leung LW, Basler CF. The role of antigen-presenting cells in filoviral hemorrhagic fever: gaps in current knowledge. Antiviral Res **2012**; 93:416–28.
5. Platanias LC. Mechanisms of type-I- and type-II-interferon-mediated signalling. Nat Rev Immunol **2005**; 5:375–86.
6. Harcourt BH, Sanchez A, Offermann MK. Ebola virus inhibits induction of genes by double-stranded RNA in endothelial cells. Virology **1998**; 252:179–88.
7. Harcourt BH, Sanchez A, Offermann MK. Ebola virus selectively inhibits responses to interferons, but not to interleukin-1beta, in endothelial cells. J Virol **1999**; 73:3491–6.
8. Gupta M, Mahanty S, Ahmed R, Rollin PE. Monocyte-derived human macrophages and peripheral blood mononuclear cells infected with

ebola virus secrete MIP-1alpha and TNF-alpha and inhibit poly-IC-induced IFN-alpha in vitro. Virology **2001**; 284:20–5.
9. Kash JC, Muhlberger E, Carter V, et al. Global suppression of the host antiviral response by Ebola- and Marburgviruses: increased antagonism of the type I interferon response is associated with enhanced virulence. J Virol **2006**; 80:3009–20.
10. Basler CF, Mikulasova A, Martinez-Sobrido L, et al. The Ebola virus VP35 protein inhibits activation of interferon regulatory factor 3. J Virol **2003**; 77:7945–56.
11. Basler CF, Wang X, Muhlberger E, et al. The Ebola virus VP35 protein functions as a type I IFN antagonist. Proc Natl Acad Sci U S A **2000**; 97: 12289–94.
12. Cardenas WB, Loo YM, Gale M Jr, et al. Ebola virus VP35 protein binds double-stranded RNA and inhibits alpha/beta interferon production induced by RIG-I signaling. J Virol **2006**; 80:5168–78.
13. Leung DW, Prins KC, Borek DM, et al. Structural basis for dsRNA recognition and interferon antagonism by Ebola VP35. Nat Struct Mol Biol **2010**; 17:165–72.
14. Reid SP, Leung LW, Hartman AL, et al. Ebola virus VP24 binds karyopherin alpha1 and blocks STAT1 nuclear accumulation. J Virol **2006**; 80: 5156–67.
15. Reid SP, Valmas C, Martinez O, Sanchez FM, Basler CF. Ebola virus VP24 proteins inhibit the interaction of NPI-1 subfamily karyopherin alpha proteins with activated STAT1. J Virol **2007**; 81:13469–77.
16. Mateo M, Reid SP, Leung LW, Basler CF, Volchkov VE. Ebolavirus VP24 binding to karyopherins is required for inhibition of interferon signaling. J Virol **2010**; 84:1169–75.
17. Xu W, Edwards MR, Borek DM, et al. Ebola virus VP24 targets a unique NLS binding site on karyopherin alpha 5 to selectively compete with nuclear import of phosphorylated STAT1. Cell Host Microbe **2014**; 16:187–200.
18. Edwards MR, Johnson B, Mire CE, et al. The Marburg virus VP24 protein interacts with Keap1 to activate the cytoprotective antioxidant response pathway. Cell Rep **2014**; 6:1017–25.
19. Valmas C, Grosch MN, Schumann M, et al. Marburg virus evades interferon responses by a mechanism distinct from ebola virus. PLoS Pathog **2010**; 6:e1000721.
20. Warfield KL, Bradfute SB, Wells J, et al. Development and characterization of a mouse model for Marburg hemorrhagic fever. J Virol **2009**; 83:6404–15.
21. Lofts LL, Wells JB, Bavari S, Warfield KL. Key genomic changes necessary for an in vivo lethal mouse marburgvirus variant selection process. J Virol **2011**; 85:3905–17.
22. Valmas C, Basler CF. Marburg virus VP40 antagonizes interferon signaling in a species-specific manner. J Virol **2011**; 85:4309–17.
23. Park MS, Garcia-Sastre A, Cros JF, Basler CF, Palese P. Newcastle disease virus V protein is a determinant of host range restriction. J Virol **2003**; 77:9522–32.
24. Best SM, Morris KL, Shannon JG, et al. Inhibition of interferon-stimulated JAK-STAT signaling by a tick-borne flavivirus and identification of NS5 as an interferon antagonist. J Virol **2005**; 79:12828–39.
25. Bray M, Davis K, Geisbert T, Schmaljohn C, Huggins J. A mouse model for evaluation of prophylaxis and therapy of Ebola hemorrhagic fever. J Infect Dis **1998**; 178:651–61.
26. Ebihara H, Takada A, Kobasa D, et al. Molecular determinants of Ebola virus virulence in mice. PLoS Pathog **2006**; 2:e73.
27. Lofts LL, Ibrahim MS, Negley DL, Hevey MC, Schmaljohn AL. Genomic differences between guinea pig lethal and nonlethal Marburg virus variants. J Infect Dis **2007**; 196(suppl 2):S305–12.
28. Volchkov VE, Chepurnov AA, Volchkova VA, Ternovoj VA, Klenk HD. Molecular characterization of guinea pig-adapted variants of Ebola virus. Virology **2000**; 277:147–55.
29. Warfield KL, Alves DA, Bradfute SB, et al. Development of a model for marburgvirus based on severe-combined immunodeficiency mice. Virol J **2007**; 4:108.
30. Feagins AR, Basler CF. The VP40 protein of Marburg virus exhibits impaired budding and increased sensitivity to human tetherin following mouse-adaptation. J Virol **2014**; 88:14440–50.